

Research Journal of Pharmaceutical, Biological and Chemical Sciences

Inhibitive Properties and Monte Carlo Simulation Studies of 5-(2-Thienyl)pyrazole on Mild Steel Corrosion in HCl Medium.

EL Aoufir Y^{1,2}, Lgaz H^{1,3}, Toumiat K⁴, Salghi R^{3*}, Jodeh S⁵, Zougagh M^{6,7}, Guenbour A², and Oudda H¹.

¹Laboratory of separation methods, Faculty of Science, Ibn Tofail University PO Box 242, Kenitra, Morocco.

²Laboratoire des matériaux, nanotechnologie et environnement. Université M^{ed}V, Rabat, Morocco.

³Laboratory of Applied Chemistry and Environment, ENSA, Ibn Zohr University, PO Box 1136, 80000 Agadir, Morocco.

⁴Department of Materials Sciences, Laghouat University, PO Box 37, 03000, Laghouat, Algeria

⁵Department of Chemistry, An-Najah National University, P. O. Box 7, Nablus, Palestine.

⁶Regional Institute for Applied Chemistry Research, IRICA, Ciudad Real, Spain

⁷Albacete Science and Technology Park, E-02006, Albacete, Spain

ABSTRACT

The corrosion inhibition effect of 5-(2-Thienyl)pyrazole (5-TPZ) on steel in 1.0 M HCl was investigated by weight loss and electrochemical methods. The effect of concentration was studied. The results indicated that the compound are efficient, mixed type and follow Langmuir adsorption isotherm and the calculated Gibbs free energy value confirms the physicochemical nature of the adsorption. *EIS* results show that the change in the impedance parameters (R_{ct} and C_{dl}) with concentrations of 5-TPZ is indicative. The adsorption of this molecule leads to the formation of a protective layer on carbon steel surface. The electrochemical results have also been supplemented by Monte Carlo simulation studies.

Keywords: Corrosion inhibition; 5-(2-Thienyl) pyrazole; Mild steel; *EIS*; Monte Carlo.

**Corresponding author*

INTRODUCTION

Acid solutions are widely used in industry, chemical cleaning, descaling, and pickling, which lead to corrosive attack. Therefore, the consumption of inhibitors to reduce corrosion has increased in recent years[1–7]. The corrosion control by inhibitors is one of the most common, effective, and economic methods to protect metals in acid media[8–13]. The majority of the well-known inhibitors are organic compounds containing heteroatoms, such as oxygen, nitrogen, or sulfur, and multiple bonds, which allow an adsorption on the metal surface[14–22]. It has been observed that the adsorption of these inhibitors depends on the physico-chemical properties of the functional groups and the electron density at the donor atom[23–27]. The adsorption occurs due to the interaction of the lone pair and/or π -orbitals of inhibitor with d-orbitals of the metal surface atoms, which evokes a greater adsorption of the inhibitor molecules onto the surface, leading to the formation of a corrosion protection film[28–30].

The objective of the present work is to investigate the inhibitor effects of 5-(2-Thienyl)pyrazole (5-TPZ) on carbon steel corrosion in 1.0 M hydrochloric acid (HCl) using weight loss, potentiodynamic polarization, Electrochemical impedance spectroscopy (EIS), and Monte Carlo simulation studies.

EXPERIMENT

Electrodes, chemicals and test solution

Corrosion tests have been performed, using the gravimetric and electrochemical measurements, on electrodes cut from sheets of carbon steel with the chemical composition: 0.370 % C, 0.230 % Si, 0.680 % Mn, 0.016 % S, 0.077 % Cr, 0.011 % Ti, 0.059 % Ni, 0.009 % Co, 0.160 % Cu, and the remainder iron.

The aggressive medium of molar hydrochloric acid used for all studies were prepared by dilution of analytical grade 37% HCl with double distilled water. The concentrations of 5-TPZ used in this investigates were varied from 10^{-4} to $5 \cdot 10^{-3}$ M. The inhibitor molecule used in this paper was purchased from Sigma–Aldrich and have the structure presented in Fig. 1. As can be seen, they have different active groups, which can act as adsorption centers.

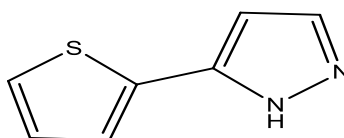


Figure 1. Chemical structure of inhibitor.

Gravimetric and electrochemical studies

Gravimetric measurements were realized in a double walled glass cell equipped with a thermostat-cooling condenser. The carbon steel specimens used have a rectangular form with dimension of $2.5 \times 2.0 \times 0.2$ cm were abraded with a different grade of emery paper (320-800-1200) and then washed thoroughly with distilled water and acetone. After weighing accurately, the specimens were immersed in beakers which contained 100 ml acid solutions without and with various concentrations of 5-TPZ at temperature equal to 303 K remained by a water thermostat for 6h as immersion time. The gravimetric tests were performed by triplicate at same conditions.

The corrosion rates (C_R) and the inhibition efficiency ($\eta_{wt} \%$) of carbon steel have been evaluated from mass loss measurement using the following equations:

$$C_R = \frac{w}{S_t} \quad (1)$$

$$\eta_{wt} \% = \frac{C_R^0 - C_R}{C_R^0} \times 100 \quad (2)$$

Where w is the average weight loss before and after exposure, respectively, S is the surface area of sample, t is the exposure time, C_R^0 and C_R is the corrosion rates of steel without and with the 5-TPZ inhibitor, respectively.

The potentiodynamic polarization curves were conducted using an electrochemical measurement system PGZ 100 Potentiostat/Galvanostat controlled by a PC supported by the Voltmaster 4.0 Software. The electrochemical measurements were performed in a conventional three electrode glass cell with carbon steel as a working electrode, platinum as counter electrode (Pt) and a saturated calomel electrode used as a reference electrode. The working electrode surface was prepared as described above gravimetric section. Prior to each electrochemical test an immersion time of 30 min was given to allow the stabilization system at corrosion potential. The polarization curves were obtained by changing the electrode potential automatically from -800 to -200 mV/SCE at a scan rate of 1 mV s⁻¹. The temperature is thermostatically controlled at desired temperature ± 1 K. The percentage protection efficiency (η_P %) is defined as:

$$\eta_{PDP}(\%) = \frac{I_{CORR}^0 - I_{CORR}}{I_{CORR}^0} \times 100 \quad (3)$$

Where, I_{CORR}^0 are corrosion current in the absence of inhibitor, I_{CORR} are corrosion current in the presence of inhibitor.

Electrochemical impedance spectroscopy (EIS) measurements were carried out with same equipment used for potentiodynamic polarization study (Voltalab PGZ 100) at applied sinusoidal potential waves of 5mV amplitudes with frequencies ranging from 100 KHz to 10 mHz at corrosion potential. The impedance diagrams are given in the Nyquist representation. The charge transfer resistance (R_{ct}) was determined from Nyquist plots and double layer capacitance (C_{dl}) was calculated from CPE parameters of the equivalent circuit deduced using Zview software. In this case the percentage protection efficiency (η_{EIS} %) is can be calculated by the value of the charge transfer resistance (R_{ct})

$$\eta_{EIS}(\%) = \frac{R_{ct} - R_{ct}^0}{R_{ct}} \times 100 \quad (4)$$

Where R_{ct}^0 and R_{ct} were the polarization resistance of uninhibited and inhibited solutions, respectively.

Monte Carlo simulation study

The Monte Carlo (MC) search was adopted to compute the low configuration adsorption energy of the interactions of the 5-TPZ on a clean iron surface. The Monte Carlo (MC) simulation was carried out using Materials Studio 6.0 software (Accelrys, Inc.)[31]. The Fe crystal was cleaved along the (110) plane, it is the most stable surface as reported in the literature. Then, the Fe (110) plane was enlarged to (8x8) supercell to provide a large surface for the interaction of the inhibitor. The simulation of the interaction between 5-TPZ and the Fe (110) surface was carried out in a simulation box (19.85 × 19.85 × 38.11 Å) with periodic boundary conditions, which modeled a representative part of the interface devoid of any arbitrary boundary effects. After that, a vacuum slab with 30 Å thickness was built above the Fe (1 1 0) plane. All simulations were implemented with the COMPASS force field to optimize the structures of all components of the system of interest. More simulation details on the methodology of Monte Carlo simulations can be found in previous publications[32–34]

RESULTS AND DISCUSSION

Weight loss study

Corrosion inhibition performance of organic compounds as corrosion inhibitors can be evaluated using electrochemical and chemical techniques. For the chemical methods, a weight loss measurement is ideally suited for long-term immersion test. The weight loss results regarding the corrosion parameters for carbon steel in 1.0 M HCl solution in the absence and presence of different concentrations of the inhibitor are summarized in Table 1. It can be seen that the corrosion rate values in 1.0 M HCl solution containing 5-TPZ, decreased as the concentration of inhibitor increased. Maximum inhibition efficiency was shown at 5.10⁻³ M of

5-TPZ. This result reveals that the compound under investigation is fairly an efficient inhibitor for carbon steel dissolution in 1.0 M HCl solution. The inhibition of corrosion of carbon steel by 5-TPZ can be explained in terms of adsorption on the metal surface[35]. This compound can be adsorbed on the carbon steel surface by the interaction between lone pairs of electrons of nitrogen, and sulfuric atoms of the inhibitor and the metal surface. This process is facilitated by the presence of vacant orbital of low energy in iron atom, as observed in the transition group elements[36,37].

Table 1: Inhibition efficiency of various concentrations of 5-TPZ for corrosion of MS in 1 M HCl obtained by weight loss measurements at 303K.

Inhibitors	Concentration (mM)	C_R ($\text{mg cm}^{-2} \text{h}^{-1}$)	η_{WL} (%)	θ
Blank	1.0	1.135	-	-
5-TPZ	5.10^{-3}	0.0434	96.18	0.9618
	1.10^{-3}	0.0677	94.03	0.9403
	5.10^{-4}	0.0985	91.32	0.9132
	1.10^{-4}	0.1266	88.84	0.8884

Polarization results

Polarization curves of the mild steel electrode in 1.0 M HCl solution at 303 K in the absence and presence of 5-TPZ are shown in Figure 2. Electrochemical parameters, i.e., corrosion potential (E_{corr}), cathodic Tafel slope (β_c) and corrosion current density (i_{corr}), obtained by extrapolation of the Tafel lines are presented in Table 2. The inhibition efficiencies (η_{PDP} %) of the compound in 1.0 M HCl are also given in Table 2.

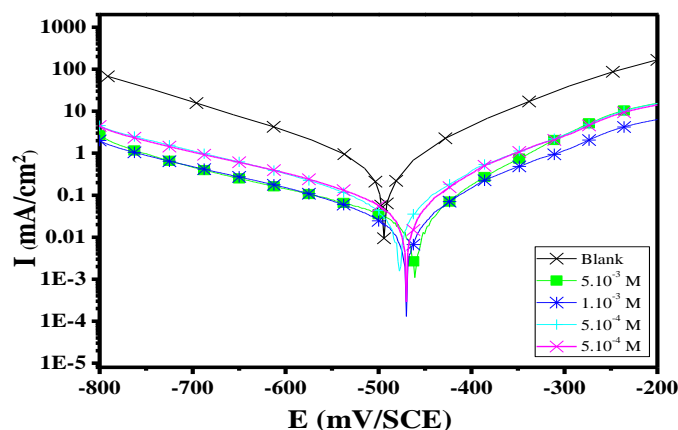


Figure 2. Polarisation curves of MS in 1 M HCl for various concentrations of 5-TPZ at 303K.

As can be seen from Figure 2, both anodic and cathodic reactions of corrosion process were significantly inhibited while the pyrazole derivative was added to the acid solution. The addition of the studied compound decreased the current densities in a large domain anodic and cathodic of potential. In literature, it has been reported that, if the displacement in E_{corr} is >85 mV with respect to E_{corr} , the inhibitor can be seen as a cathodic or anodic type and 2) if the displacement in E_{corr} is <85 mV, the inhibitor can be seen as mixed type[38,39]. In our study, the maximum displacement in E_{corr} value is 32.8 mV towards anodic region, which indicates that studied pyrazole derivative is mixed-type inhibitor. The increase in inhibition efficiency with increasing inhibitor concentration may be attributed to the formation of a barrier film, which prevents the attack of acid on the metal surface[37,40,41]. It can be observed from Table 2 that the i_{corr} values decrease considerably in the presence of 5-TPZ and the i_{corr} values have a trend to decrease with the increasing inhibitor concentration. Correspondingly, inhibition efficiencies (η_{PDP} %) values increase with the increasing inhibitor concentration and then reach a maximum value at 5 mM.

Table 2. Corrosion parameters for corrosion of MS with selected concentrations of 5-TPZ in 1 M HCl by Potentiodynamic polarization method at 303K.

Inhibitor	Concentration (M)	$-E_{corr}$ (mV/SCE)	$-\beta_c$ (mV dec ⁻¹)	i_{corr} ($\mu\text{A cm}^{-2}$)	η_{PDP} (%)	Θ
Blank	-	496	162.0	564.0	-	-
5-TPZ	5.10^{-3}	463.2	195.6	25.21	95.53	0.9553
	1.10^{-3}	472.5	193.4	35.08	93.78	0.9378
	5.10^{-4}	480.5	164.9	55.3	90.19	0.9019
	1.10^{-4}	474.1	191.3	78	86.17	0.8617

Electrochemical impedance spectroscopy (EIS)

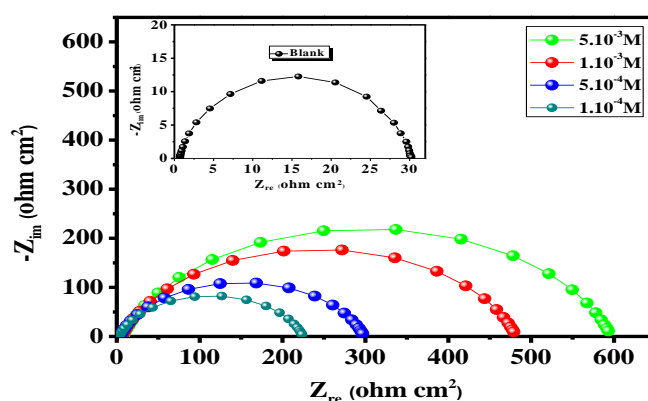
Electrochemical impedance spectroscopy (EIS) is a well-established and powerful tool in the study of corrosion. Surface properties, electrode kinetics, and mechanistic information can be obtained from the impedance diagrams[42]. Figure 3, shows the Nyquist plots obtained at the open circuit potential after immersion for 0.5 h. Table 3 summarizes the impedance data extracted from EIS experiments carried out both in the absence and presence of increasing concentrations of 5-TPZ. Semicircular appearance of Nyquist plots shows that the charge-transfer process takes place during dissolution[43,44]. From the curves, it is clear that the impedance response for carbon steel in uninhibited acid solution has significantly changed after the addition of inhibitor. The impedance spectra were fitted to the $R_s(R_{ct}CPE)$ equivalent circuit of the form in Fig. 4. Where R_s is the solution resistance, R_{ct} denotes the charge-transfer resistance and CPE is constant phase element. The introduction of CPE into the circuit was necessitated to explain the depression of the capacitance semicircle, which corresponds to surface heterogeneity resulting from surface roughness, impurities, and adsorption of inhibitors[36,37,41]. The impedance of this element is frequency-dependent and can be calculated using the Eq. 5:

$$Z_{CPE} = \frac{1}{Q(j\omega)^n} \quad (5)$$

Where Q is the CPE constant (in $\Omega^{-1} \text{S}^n \text{cm}^{-2}$), ω is the angular frequency (in rad s^{-1}), $j^2 = -1$ is the imaginary number and n is a CPE exponent which can be used as a gauge for the heterogeneity or roughness of the surface[45,46]. In addition, the double layer capacitances, C_{dl} , for a circuit including a CPE were calculated by using the following Eq. 6:

$$C_{dl} = (Q \cdot R_{ct}^{1-n})^{1/n} \quad (6)$$

The fact that the impedance diagrams have an approximately semicircular appearance shows that a charge-transfer process controls the corrosion of carbon steel in 1.0 M HCl.


Figure 3. Nyquist curves for mild steel in 1M HCl for selected concentrations of 5-TPZ at 303K.

By increasing the inhibitor concentrations, the R_{ct} values increase and the C_{dl} values decrease, which causes an increase in inhibition efficiency. The most pronounced effect and the highest R_{ct} is obtained by concentration 5.10^{-3} M of the inhibitor. The decrease in C_{dl} can result from the decrease of the local dielectric constant and/or from the increase of thickness of the electrical double layer, which suggests an adsorption of the inhibitor molecules on the carbon steel surface[47,48]. The thickness of the protective layer δ , is related to C_{dl} by the following equation:

$$\delta = \frac{\epsilon_0 \epsilon_r}{C_{dl}} \quad (7)$$

where ϵ_0 is the dielectric constant and ϵ_r is the relative dielectric constant. McCafferty and Hackerman[49] attributed the change in C_{dl} values to the gradual replacement of water molecules by the adsorption of the organic molecules on the metal surface, decreasing the extent of metal dissolution. The impedance data confirm the inhibition behavior of the inhibitor with that obtained from other techniques. It can be concluded that the inhibition efficiency found from weight loss, polarization curves, and electrochemical impedance spectroscopy measurements are in good agreement.

Table 3. AC-impedance parameters for corrosion of mild steel for selected concentrations of 5-TPZ in 1M HCl at 303K.

Inhibitor	Concentration (M)	R_{ct} (Ω cm ²)	n	$Q \times 10^{-4}$ ($s^n \Omega^{-1} \text{cm}^{-2}$)	C_{dl} ($\mu\text{F cm}^{-2}$)	η_{EIS} (%)	θ
Blank	1.0	29.35	0.910	1.7610	91.6	-	-
5-TPZ	5.10^{-3}	589.7	0.892	0.1688	9.66	95.02	0.9502
	1.10^{-3}	476.3	0.864	0.2667	13.41	93.83	0.9383
	5.10^{-4}	294.8	0.874	0.3777	19.74	90.04	0.9004
	1.10^{-4}	222.3	0.883	0.4823	26.44	86.79	0.8679

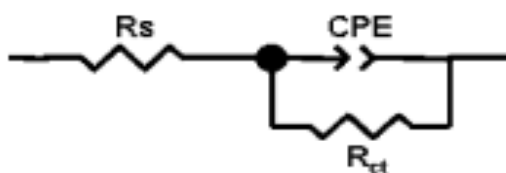


Figure 4. Equivalent electrical circuit corresponding to the corrosion process on the carbon steel in hydrochloric acid.

Adsorption isotherm

The proposed adsorption of the pyrazole derivative was further characterized by fitting the surface coverage (θ) data obtained gravimetrically to the Langmuir isotherm[8,9]:

$$\frac{C}{\theta} = \frac{1}{K_{ads}} + C \quad (8)$$

Where, C is the concentration of the inhibitor, K_{ads} is the equilibrium constant of adsorption and θ is the surface coverage. The Langmuir approach is based on a molecular kinetic model of the adsorption–desorption process. On the other hand, the adsorption equilibrium constant (K_{ads}) is related to the standard free energy of adsorption (ΔG°_{ads}) of the inhibitor molecules by the following Eq. 9[9]:

$$K_{ads} = \frac{1}{55.5} \exp\left(\frac{-\Delta G^{\circ}_{ads}}{RT}\right) \quad (9)$$

Where R is the universal gas constant, T the absolute temperature in K, and 55.5 represents the molar concentration of water in the solution. It generally accepted that the values of ΔG°_{ads} up to -20 kJ mol⁻¹,

the types of adsorption were regarded as physisorption, the inhibition acts due to the electrostatic interaction

between the charged molecules and the charged metal. While the values around -40 kJ mol^{-1} or smaller, were seen as chemisorption, which is due to the charge sharing or a transfer from the inhibitor molecules to the metal surface to form covalent bond[37]. In this study, the free energy of adsorption ΔG_{ads}° and the adsorption

equilibrium constant (K_{ads}) are found to be $-37.17 \text{ kJ mol}^{-1}$ and 46591 M^{-1} , respectively. The higher value of K_{ads} and the negative and low value of ΔG_{ads}° indicate the spontaneous adsorption of the inhibitor and have strong

interaction with the metal surface[41]. It suggested that the adsorption mechanism of the 5-TPZ on carbon steel in 1.0 M HCl solution was typical of physical and chemical adsorptions[35,36].

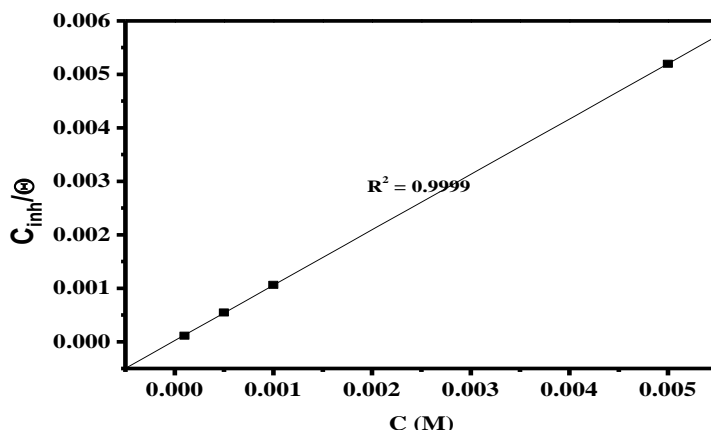


Figure 5: Langmuir adsorption of inhibitor on the MS surface in 1.0 M HCl solution at 303K.

Molecular dynamic (Monte Carlo) simulation

To investigate the adsorption mechanism of the studied compound on the steel surface, the adsorption of 5-TPZ was studied theoretically by using Monte Carlo simulation methods. As can be seen in Table 4 present the outputs and descriptors calculated by the Monte Carlo simulation. Figure 6 shows the most suitable configurations for adsorption of 5-TPZ on Fe (1 1 0) substrate obtained by Monte Carlo simulation. The adsorption energy of 5-TPZ is more than $-90 \text{ kcal mol}^{-1}$ which explain its highest inhibition efficiency. High values of adsorption density presented in Figure 6 indicates that 5-TPZ is likely to adsorb on the iron surface to form stable ad layers and protect iron from corrosion[33,34].

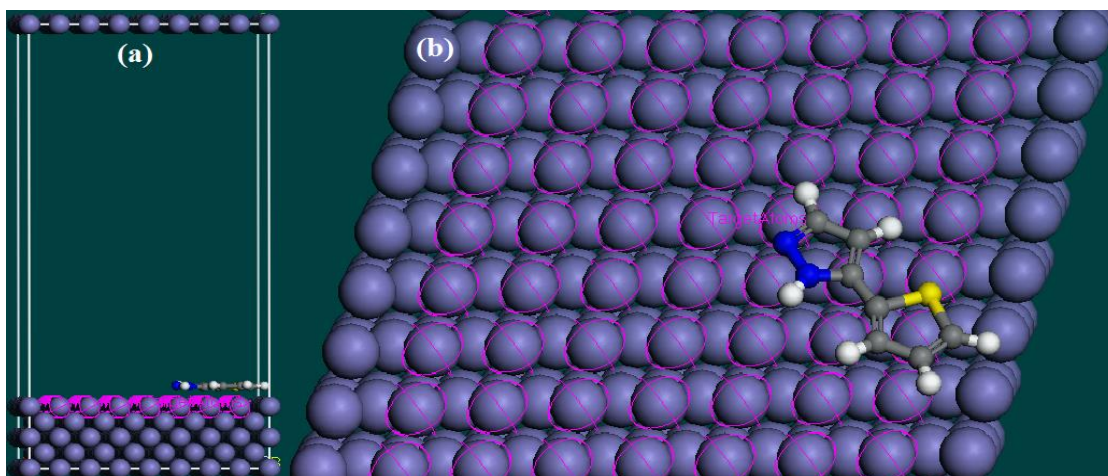


Figure 6. The most stable low energy configuration for the adsorption of the inhibitor on Fe (1 1 0) surface obtained through the Monte Carlo simulation.(a) side view, (b) top view.

Table 4: Outputs and descriptors calculated by the Monte Carlo simulation for the lowest adsorption configurations of 5-TPZ on Fe (1 1 0) surface (in kcal/mol).

System	Total energy	Adsorption energy	Rigid adsorption energy	Deformation energy	dEad/dNi inhibitor
Fe (1 1 0)/5-TPZ	21.312	-90.846	-91.480	0.633	-84.231

CONCLUSION

Corrosion inhibition properties of 5-TPZ were investigated on mild steel in 1 M HCl using electrochemical methods, weight loss and Monte Carlo simulations. The following conclusions were drawn from the results:

- ✓ The inhibitor studied in this work showed appreciable inhibition efficiency for mild steel corrosion in 1 M HCl and the inhibition efficiency increases with increasing concentration of the inhibitor.
- ✓ Potentiodynamic polarization study showed that the studied pyrazole derivative is mixed type inhibitor and the *EIS* study revealed that the 5-TPZ form protective film on mild steel surface.
- ✓ The experimental results showed that the studied compound adsorb spontaneously on mild steel surface and conform to the Langmuir adsorption isotherm. The adsorption process involves both physisorption and chemisorption mechanisms.
- ✓ Both experimental and Monte Carlo simulations results showed that the 5-TPZ act as efficient inhibitor for mild steel in 1 M HCl medium.

ACKNOWLEDGEMENTS

Financial support from the Spanish Ministry of Science and Innovation (CTQ2010-61830) is gratefully acknowledged. The support given through a "INCRECYT" research contract to M. Zougagh.

REFERENCES

- [1] Adardour L, Larouj M, Lgaz H, Belkhaouda M, Salghi R, Jodeh S, et al. *Pharma Chem* 2016;8:152–60.
- [2] Afia L, Larouj M, Lgaz H, Salghi R, Jodeh S, Samhan S, et al. *Pharma Chem* 2016;8:22–35.
- [3] Afia L, Larouj M, Salghi R, Jodeh S, Zougagh M, Rasem Hasan A, et al. *Pharma Chem* 2016;8:166–79.
- [4] Bousskri A, Salghi R, Anejjar A, Jodeh S, Quraishi MA, Larouj M, et al. *Pharma Chem* 2016;8:67–83.
- [5] El Makrini B, Larouj M, Lgaz H, R. Salghi, Salman A, Belkhaouda M, et al. *Pharma Chem* 2016;8:227–37.
- [6] El Makrini B, Lgaz H, Larouj M, Salghi R, Rasem Hasan A, Belkhaouda M, et al. *Pharma Chem* 2016;8:256–68.
- [7] Larouj M, Belkhaouda M, Lgaz H, Salghi R, Jodeh S, Samhan S, et al. *Pharma Chem* 2016;8:114–33.
- [8] Larouj M, Lgaz H, Houda S, Zarrok H, Zarrouk A, Elmidaoui A, et al. *J Mater Environ Sci* 2015;6:3251–67.
- [9] Lgaz H, Benali O, Salghi R, Jodeh S, Larouj M, Hamed O, et al. *Pharma Chem* 2016;8:172–90.
- [10] Lgaz H, ELaoufir Y, Ramli Y, Larouj M, Zarrok H, Salghi R, et al. *Pharma Chem* 2015;8:36–45.
- [11] Lgaz H, Belkhaouda M, Larouj M, Salghi R, Jodeh S, Warad I, et al. *Mor J Chem* 2016;4:101–11.
- [12] Lotfi N, Lgaz H, Belkhaouda M, Larouj M, Salghi R, Jodeh S, et al. *Arab J Chem Environ Res* 2014;1:13–23.
- [13] Lotfi N, Lgaz H, Belkhaouda M, Larouj M, Salghi R, Jodeh S, et al. *Arab J Chem Environ Res* 2015;1:13–23.
- [14] Adardour L, Lgaz H, Salghi R, Larouj M, Jodeh S, Zougagh M, et al. *Pharm Lett* 2016;8:126–37.
- [15] Adardour L, Lgaz H, Salghi R, Larouj M, Jodeh S, Zougagh M, et al. *Pharm Lett* 2016;8:173–85.
- [16] Adardour L, Lgaz H, Salghi R, Larouj M, Jodeh S, Zougagh M, et al. *Pharm Lett* 2016;8:212–24.
- [17] Saadouni M, Larouj M, Salghi R, Lgaz H, Jodeh S, Zougagh M, et al. *Pharm Lett* 2016;8:65–76.
- [18] Saadouni M, Larouj M, Salghi R, Lgaz H, Jodeh S, Zougagh M, et al. *Pharm Lett* 2016;8:96–107.
- [19] Lgaz H, Anejjar A, Salghi R, Jodeh S, Zougagh M, Warad I, et al. *Int J Corros Scale Inhib* 2016;5:209–231.
- [20] Lgaz H, Salghi R, Larouj M, Elfaydy M, Jodeh S, About H, et al. *Mor J Chem* 2016;4:592–612.

- [21] Larouj M, Lgaz H, Salghi R, Jodeh S, Messali M, Zougagh M, et al. *Mor J Chem* 2016;4:567–83.
- [22] Larouj M, Lgaz H, Salghi R, Oudda H, Jodeh S, Chetouani A. *Mor J Chem* 2016;4:425–36.
- [23] Ahamad I, Quraishi M. *Corros Sci* 2010;52:651–6.
- [24] Benabdellah M, Aouniti A, Dafali A, Hammouti B, Benkaddour M, Yahyi A, et al. *Appl Surf Sci* 2006;252:8341–7.
- [25] Cao Z, Tang Y, Cang H, Xu J, Lu G, Jing W. *Corros Sci* 2014;83:292–8.
- [26] Düdükçü M, Yazici B, Erbil M. *Mater Chem Phys* 2004;87:138–41.
- [27] Ebenso EE, Kabanda MM, Murulana LC, Singh AK, Shukla SK. *Ind Eng Chem Res* 2012;51:12940–58.
- [28] Fouda A, Elewady G, Shalabi K, El-Aziz HA. *RSC Adv* 2015;5:36957–68.
- [29] Galal A, Atta N, Al-Hassan M. *Mater Chem Phys* 2005;89:38–48.
- [30] Gasparac R, Martin C, Stupnisek-Lisac E. *J Electrochem Soc* 2000;147.
- [31] *Materials Studio. Revision 6.0. Accelrys Inc., San Diego, USA; 2013.*
- [32] Eivani AR, Zhou J, Duszczek J. *Comput Mater Sci* 2012;54:370–7. doi:10.1016/j.commatsci.2011.10.016.
- [33] Hmamou DB, Salghi R, Zarrouk A, Zarrok H, Touzani R, Hammouti B, et al. *J Environ Chem Eng* 2015;3:2031–41. doi:10.1016/j.jece.2015.03.018.
- [34] Kaya S, Tüzün B, Kaya C, Obot IB. *J Taiwan Inst Chem Eng* 2016;58:528–35. doi:10.1016/j.jtice.2015.06.009.
- [35] Verma C, Olasunkanmi L, Obot I, Ebenso EE, Quraishi M. *RSC Adv* 2016;6:15639–54.
- [36] Verma C, Quraishi MA, Olasunkanmi LO, Ebenso EE. *RSC Adv* 2015;5:85417–30. doi:10.1039/C5RA16982H.
- [37] Yadav DK, Maiti B, Quraishi M. *Corros Sci* 2010;52:3586–98.
- [38] ElBelghiti M, Karzazi Y, Dafali A, Hammouti B, Bentiss F, Obot I, et al. *J Mol Liq* 2016;218:281–93.
- [39] Elmsellem H, Youssef MH, Aouniti A, Hadda TB, Chetouani A, Hammouti B. *Russ J Appl Chem* 2014;87:744–53. doi:10.1134/S1070427214060147.
- [40] Yıldız R, Doğan T, Dehri I. *Corros Sci* 2014;85:215–21.
- [41] Yadav M, Sinha R, Kumar S, Sarkar T. *RSC Adv* 2015;5:70832–48.
- [42] Lorenz W, Mansfeld F. *Corros Sci* 1981;21:647–72.
- [43] Hosseini M, Ehteshamzadeh M, Shahrabi T. *Electrochimica Acta* 2007;52:3680–5.
- [44] Lebrini M, Robert F, Lecante A, Roos C. *Corros Sci* 2011;53:687–95. doi:10.1016/j.corsci.2010.10.006.
- [45] Amin MA, Ahmed M, Arida H, Arslan T, Saracoglu M, Kandemirli F. *Corros Sci* 2011;53:540–8.
- [46] Amin MA, El-Rehim SA, El-Sherbini E, Bayoumi RS. *Int J Electrochem Sci* 2008;3:199–215.
- [47] El-Rehim SA, Refaey S, Taha F, Saleh M, Ahmed R. *J Appl Electrochem* 2001;31:429–35.
- [48] Fan H-B, Fu C-Y, Wang H-L, Guo X-P, Zheng J-S. *Br Corros J* 2002;37:122–5.
- [49] McCafferty E, Hackerman N. *J Electrochem Soc* 1972;119:146–54.